Report Number
I-62-3

Effects of Radial Energy Release Variations on Transverse Combustion Pressure Oscillations

by

J. R. Osborn and J. R. Rahon

Interim Report No. 5
Contract N onr 1100 (21)
March 1962

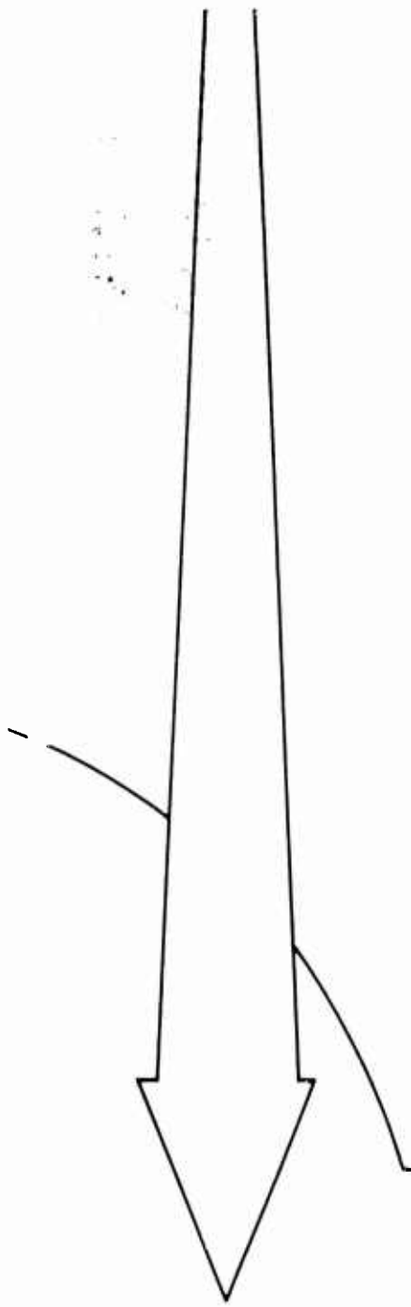

JET PROPULSION CENTER
PURDUE UNIVERSITY

SCHOOL OF MECHANICAL ENGINEERING
LAFAYETTE, INDIANA

PURDUE UNIVERSITY

AND

PURDUE RESEARCH FOUNDATION

Lafayette, Indiana

Report No. I-62-3

EFFECTS OF RADIAL ENERGY RELEASE VARIATIONS ON TRANSVERSE COMBUSTION PRESSURE OSCILLATIONS

by

J. R. Osborn and J. R. Rahon

Interim Report No. 5

Contract N onr 1100(21)

Jet Propulsion Center

Purdue University

March 1962

ACKNOWLEDGMENTS

The authors wish to thank Dr. M. J. Zucrow, Atkins Professor of Engineering, Purdue University, for helpful guidance and counsel throughout the course of the investigation. The authors are also grateful to Mr. J. M. Bonnell for his helpful assistance and suggestions and to Mr. A. Akpinar for his assistance in the collecting and reduction of the data.

Acknowledgment is also given to the Office of Naval Research, Contract N onr 1100(21), under whose sponsorship the research reported herein was conducted. Reproduction in full or in part is permitted for any use of the United States Government.

TABLE OF CONTENTS

TABLE OF CONTENTS (Continued)

LIST OF ILLUSTRATIONS

ABSTRACT

A gaseous bipropellant rocket motor was operated utilizing ethylene and air. The motor was of fixed geometry and had an injector which provided for controlled proportions of the total propellant flow to be injected at various radial locations. Operation was accomplished with three types of energy release distribution and the resultant oscillations observed and recorded.

It was determined that the mode and severity of the observed transverse combustion pressure oscillations were a function of the location of the energy release (propellant injection) and the frequency of the excited modes. From these observations, it was concluded that a balance could be achieved wherein two modes could be excited with equal vigor and their resultant interaction would produce stable operation.

INTRODUCTION

In the operation of rocket motors, variations in the combustion pressure about the mean design value may occur. These variations may be random or periodic, the random type being termed rough burning and the periodic being termed oscillatory burning. Oscillatory burning has been generally divided into low frequency, from approximately 30 to 500 cycles per second, and high frequency, from approximately 1000 to perhaps 20,000 cycles per second.

The low frequency oscillations are attributed to an interaction between the dynamic properties of the combustion process and the dynamic characteristics of the propellant feed lines and injector (1)*. The high frequency oscillations are related to the resonant acoustical modes in the combustion chamber and thus may be of the longitudinal mode or of the transverse modes depending upon the geometry of the chamber (2).

The high frequency modes are sustained by the energy released in the combustion chamber during the combustion process. It has been found that the location of this energy release is closely related to the mode and amplitude of the oscillations that occur (5).

The object of the series of experiments discussed herein is to provide a well defined energy release profile across the injector face in a rocket motor susceptible to transverse oscillations, in an effort to determine

---

* Numbers in parentheses are References listed in the Bibliography.

the effects of these various energy release profiles on the inherent instability of the motor.

METHOD OF INVESTIGATION

General Discussion

An experimental investigation was conducted with the rocket motor shown in Fig. 1. Premixed ethylene and air were the propellants utilized. The combustion chamber length was 6 inches and the inside diameter was 7 inches, the nozzle throat diameter being 0.5 inches.

Propellant flow was controlled during the operation of the rocket motor by regulators in the propellant feed lines. By adjusting the settings of these regulators, the operator was able to control the operating conditions of mean chamber pressure and equivalence ratio.*

Capabilities of the propellant feed system determined the ranges of mean chamber pressure and equivalence ratio obtained. The range of mean chamber pressure was from approximately 30 psia to 200 psia, while that of the equivalence ratio was from the lower inflammability limit, (equivalence ratio approximately equal to 0.5) to approximately 2.0.

Mean chamber pressure, the pressure drops across the propellant metering orifices and the pressures and temperatures upstream of these orifices were automatically recorded for each datum point.

High frequency periodic oscillations of the combustion pressure were converted to an analogous voltage by a Photocon-Dynagage system. This voltage was recorded by an Ampex tape recorder. The amplitude and frequency were determined by comparison of the experimental signal with a signal of

---

* Equivalence ratio is defined as the ratio of the actual fuel-oxidizer ratio divided by the stoichiometric fuel-oxidizer ratio.

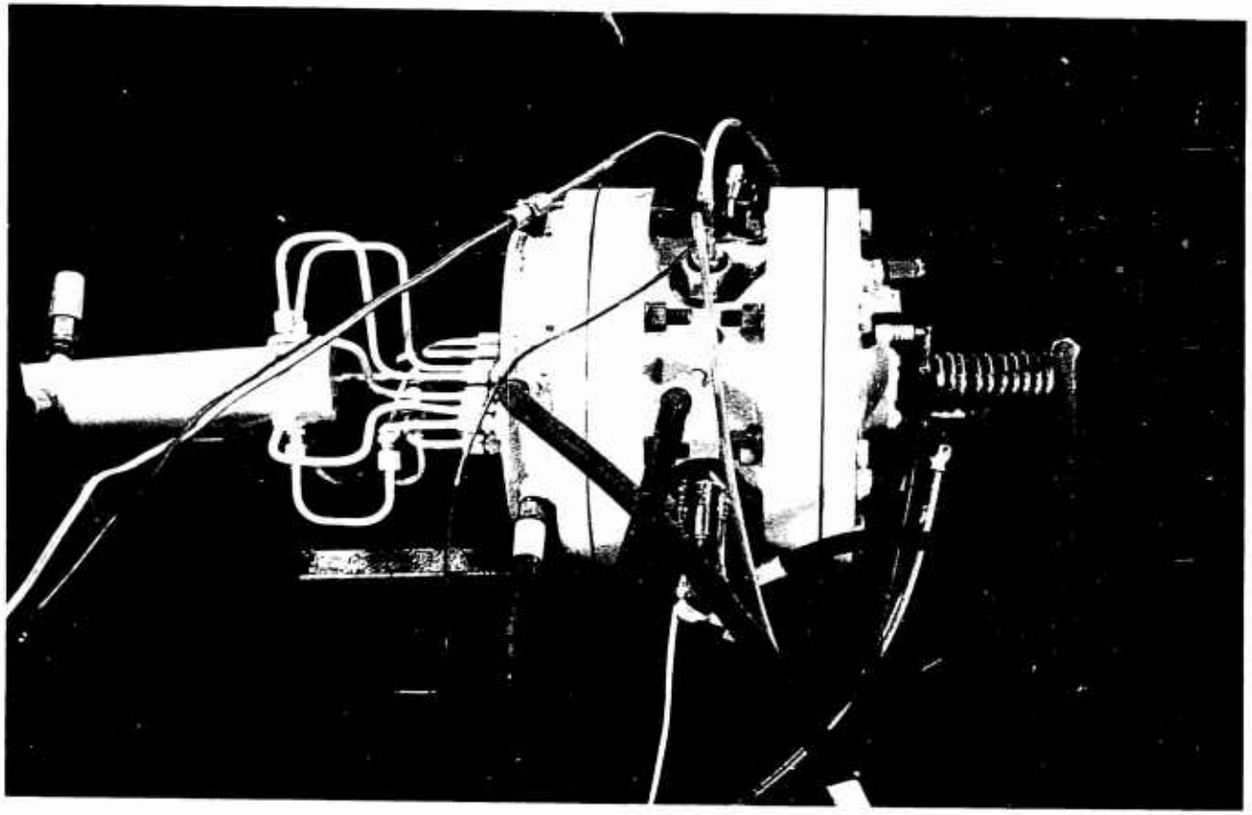

FIG. 1 ROCKET MOTOR INSTALLATION

known amplitude and frequency. More detailed information concerning the apparatus and data reduction is given in Appendices C and D and Reference 5.

For each datum point, the following information was obtained:

(1) mean chamber pressure,

(2) equivalence ratio,

(3) frequency of combustion pressure oscillations,

(4) peak-to-peak amplitude of oscillations, and

(5) mode of oscillations.

For each of the injection schemes described below, sufficient data were obtained to determine an instability region (see Fig. 4 for a typical region). Results for each of the injection schemes were then compared to each other and to the applicable results of other investigators (5, 7, 11). Conclusions were then drawn concerning the effects of energy release location, frequency and mode of oscillation, and the interdependence of these effects.

Method of Propellant Injection

Three methods of energy release were utilized in the course of the experimental work. These shall be referred to as Energy Release Profiles I, II, and III, and they are shown in Fig. 2. Profile I has a constant amount of energy release as a function of combustion chamber radius, profile II has a decreasing amount with increasing radius, while profile III is such that the amount of energy released increases linearly with radius.

During the course of this investigation, the assumption has been made that the energy release profile is proportional to the amount of propellant injected per unit of injector face area. This assumption is justified by

PARAMETERS MAINTAINED CONSTANT:

MOTOR DIAMETER	7 in.
MOTOR LENGTH	6 in.
PROPELLANTS	ETHYLENE - AIR (PREMIXED)
NOZZLE DIAMETER	0.5 in.

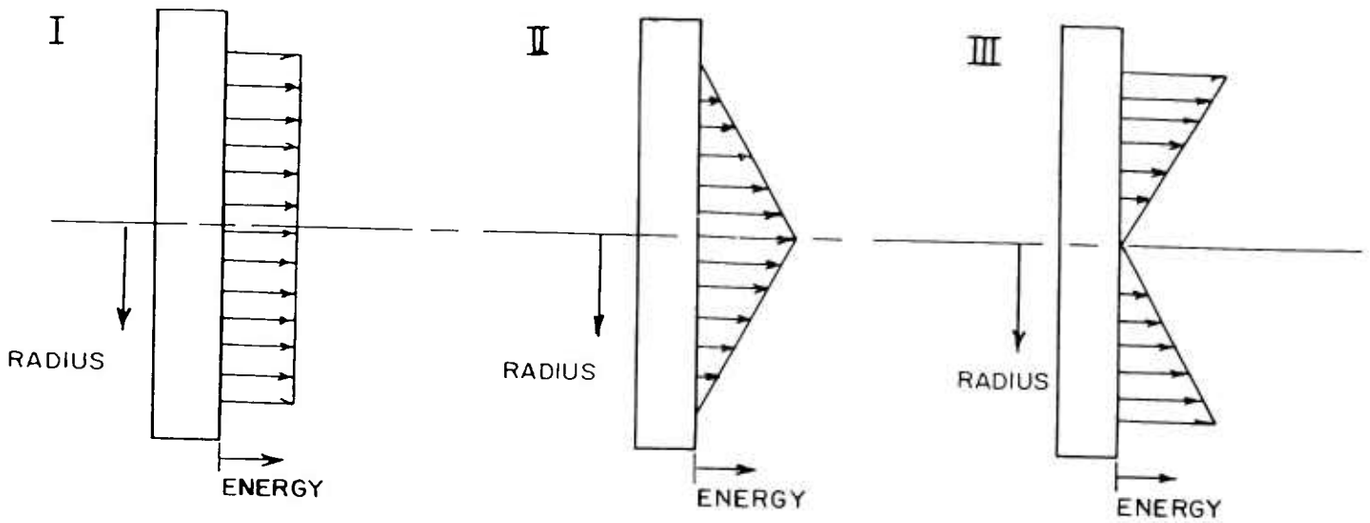

FIG. 2 ENERGY RELEASE PROFILES

two considerations. First, since the propellants are premixed before injection, they burn (thus releasing energy) very close to the injector face, the time necessary for the physical mixing being longer than the actual burning time (3). Second, since only the transverse modes are under investigation, the radial location of the energy release is significant while the axial location is relatively unimportant. This means that the assumption is valid unless the diffusion of the propellants from one radial location to another, admittedly a slow process, takes place more rapidly than the combustion process.

Occurrence of only the transverse modes was assured by selecting the length of the combustion chamber below the lower critical length* for the ethylene-air propellant combination (2).

---

* The lower critical length is that length, for a given propellant combination, below which no oscillations of the longitudinal mode will occur. For ethylene and air it is 6 inches.

EXPERIMENTAL RESULTS

Instability Regions

Figure 3 depicts a typical instability region. An instability region is a map of all the operating points for a particular rocket motor-injector configuration. Its coordinates are mean combustion chamber pressure and equivalence ratio. Since the region contains all operating points, it can be divided into sub-regions of stable and unstable operation. The sub-regions of unstable operation can be subdivided into smaller regions, each of which comprises an area of constant peak-to-peak amplitude of combustion pressure oscillation. Instability regions are a convenient and comprehensive graphical manner for plotting the data obtained from the operation of a rocket motor configuration. The data obtained in the experimental work discussed herein will be presented in this form.

Profile I

Figure 3 is the instability region plotted from the data obtained from the experimental work employing profile I. Operation with profile I resulted in a narrow region of instability between equivalence ratios of 0.5 and 0.6. The lowest mean chamber pressure at which oscillations occurred was approximately 80 psia.

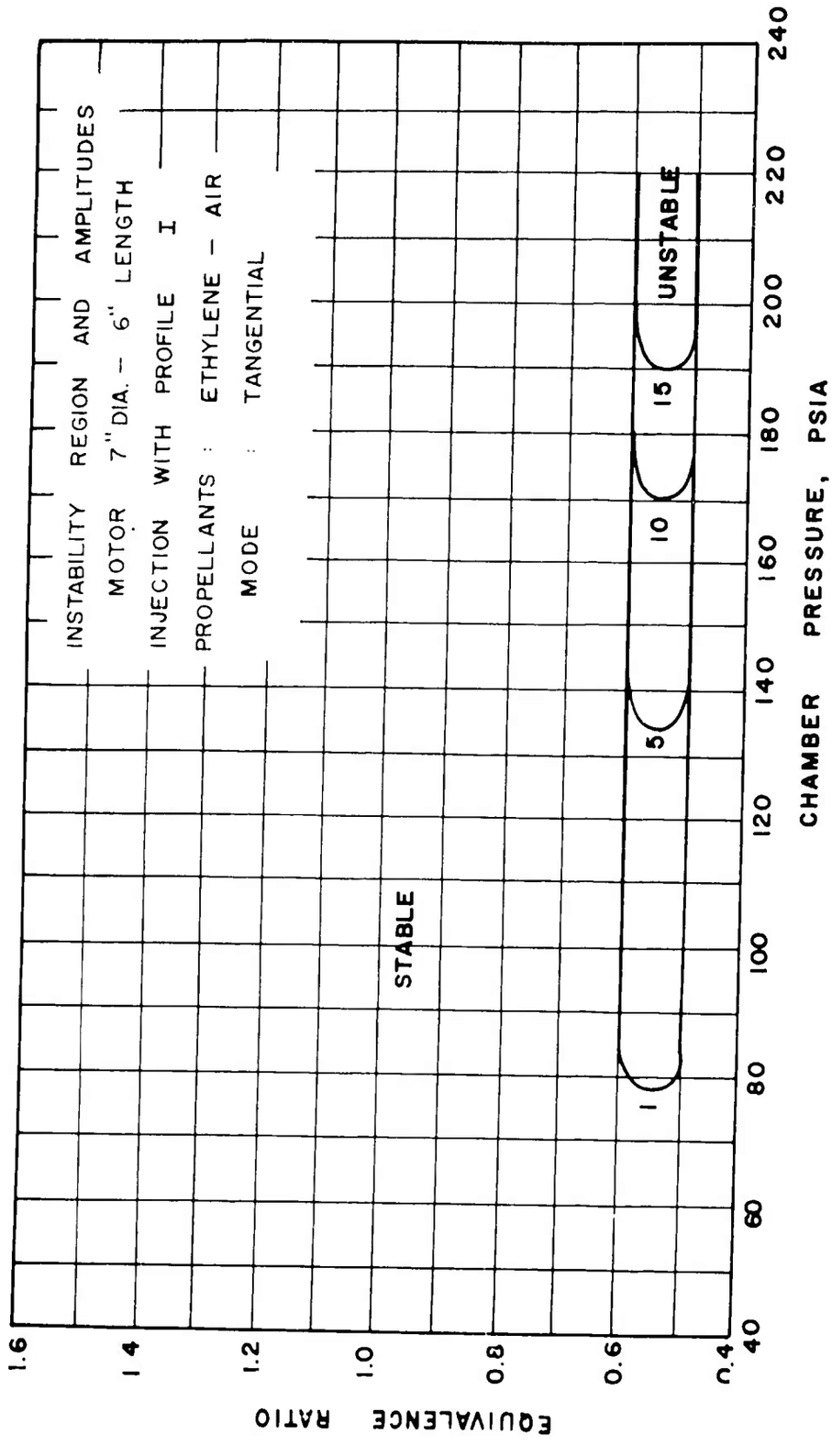

FIG. 3 INSTABILITY REGION OF PROFILE I

Profile II

Operation with profile II resulted in essentially stable operation over the entire range of mean combustion chamber pressure and equivalence ratio investigated. Thus, no instability region is presented. The range of mean chamber pressure was from about 30 psia to approximately 200 psia. Equivalence ratios investigated ranged from the lower inflammability limit (equivalence ratio approximately equal to 0.5) to about 2.0.

In several isolated instances, low amplitude oscillations were observed; these were of a transient nature only. These observations were random in occurrence and could not be employed for establishing an instability region.

Profile III

Operation of the rocket motor system with the injector having energy release profile III resulted in the instability regions presented in Fig. 4. There was a narrow region of instability at low equivalence ratios (from 0.5 to 0.7) that was quite similar to that of profile I. For profile III the lowest mean chamber pressure at which oscillations occurred was approximately 105 psia, and the observed oscillations were weaker than those at similar operating points for profile I. For example, at an equivalence ratio of 0.55 and a mean chamber pressure of 170 psia, profile III exhibited oscillations of about 15 psi while those observed with profile I were approximately 10 psi.

In addition, there was another region located at equivalence ratios of 1.2 and above. The lowest mean chamber pressure at which oscillations in this region occurred was 140 psia. At any mean chamber pressure, the

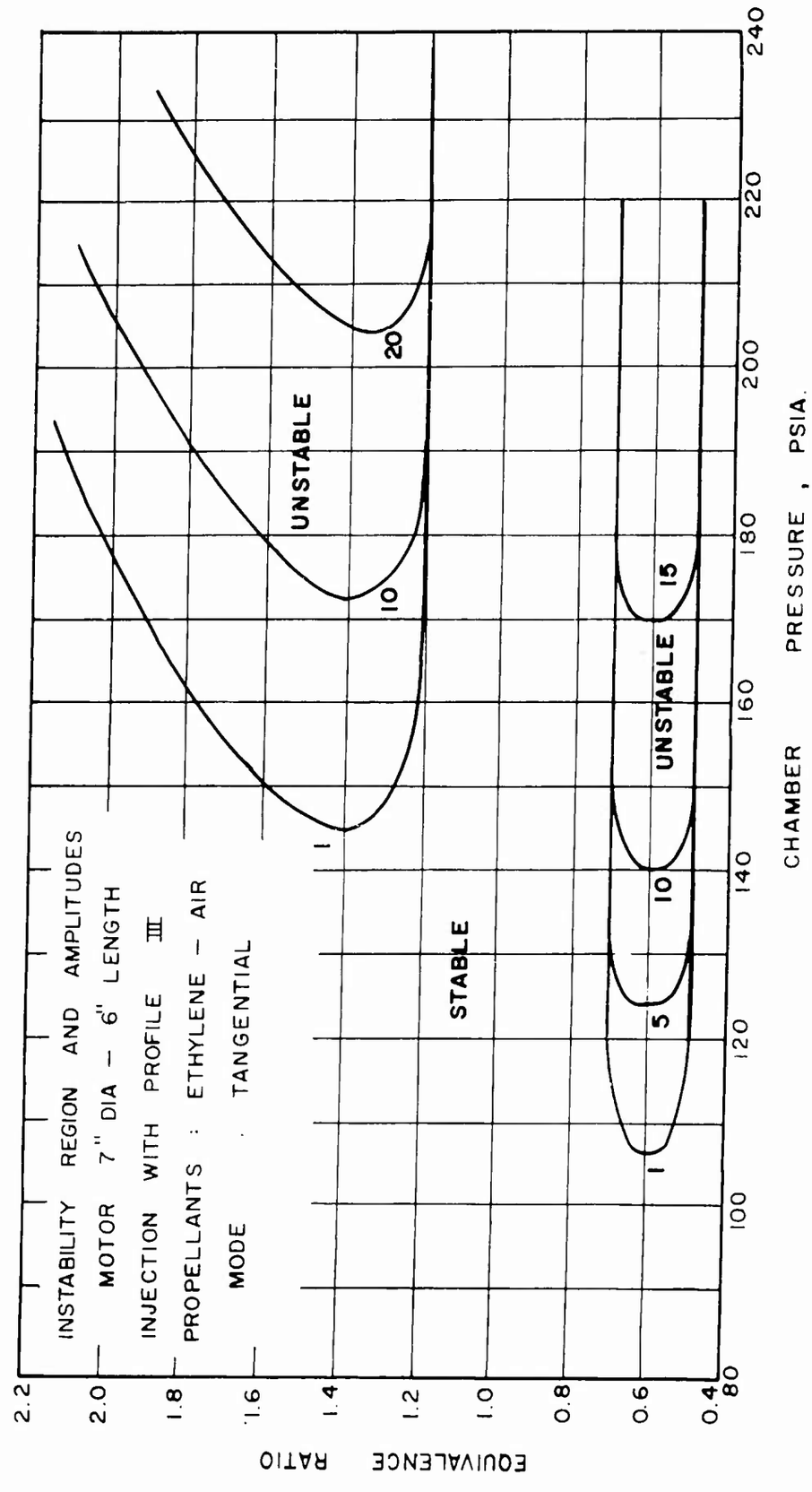

FIG. 4 INSTABILITY REGIONS OF PROFILE III

oscillations that occurred in the lower region were always of higher amplitude than those in the upper region. For example, at a mean chamber pressure of 170 psia, the maximum amplitude of oscillation in the low region was 15 psi while that in the upper region was only 10 psi.

Modes of Oscillation

Determination of Modal Types

The modes of a transverse combustion pressure oscillation can be determined by either of two methods. The first method consists of strategically locating several transducers in the combustion chamber wall (see Reference 6). From the phase relationship of the resultant signals obtained from those transducers, the mode of oscillation can be determined.

The second method consists of computing a theoretical frequency of oscillation for the different acoustic modes and comparing this to the frequency obtained in the experiments. The frequency of the various modes may be calculated according to acoustical theory (2, 5).

In this series of experiments, mode identification was accomplished by the latter method. The following acoustic frequencies are those calculated for the motor geometry and propellant combination under consideration (2, 5):

Table 1

Theoretical Acoustical Frequencies

	E.R.* = 1	E.R. = 0.5
First radial mode	6300 cps	5220 cps
First tangential mode	3200 cps	2510 cps
First spinning mode	3200 cps	2510 cps
Second radial mode	11250 cps	9550 cps
Second tangential mode	4900 cps	4160 cps
Second spinning mode	4900 cps	4160 cps

* E.R. is an abbreviation for equivalence ratio.

Profile I

For this profile, the frequency of the oscillations was in the range from 2400 to 2500 cps. The region of instability occurred at low equivalence ratios (0.5 to 0.6). Since the theoretical frequency for the first tangential mode, in that equivalence ratio range, is approximately the same value, 2510 cps (see Table 1), it was concluded that the observed oscillations were of the first tangential mode.

Profile II

The isolated instances of instability previously noted for this profile were of various modes, the first and second tangential, and the first radial all being represented. This random occurrence further contributed to the conclusion that the few oscillations observed were transient in nature and should be disregarded.

Profile III

While the equivalence ratio of the observed oscillations varied from 0.5 to approximately 2.0, the frequency of the oscillations varied from about 2300 cps at the lower ratios to approximately 3000 cps at the higher values. By comparison of these values with the theoretical frequencies given above it was concluded that the observed oscillations of profile III were the first tangential mode.

Peak-to-Peak Amplitudes

Rating of the three profiles with respect to severity of oscillation was accomplished by considering the peak-to-peak amplitude of the oscillations for each of the profiles when operated under identical conditions of mean chamber pressure and equivalence ratio.

Profile II exhibited only random, weak oscillations and thus is considered essentially stable over the entire operating range. In the narrow region of instability at low equivalence ratios (0.5 to 0.7), profile III has higher amplitudes than profile I (15 psi as compared to 10 psi at a mean chamber pressure of 170 psia). One exception is known, a small portion of the instability region at chamber pressures below approximately 110 psia. Since profile III exhibited an unstable region at high equivalence ratios (above 1.2) and also had stronger oscillations at common points of instability as shown above, it is considered more unstable than profile I. Thus, the order of decreasing severity of unstable operation for the three injection profiles would be profile III, profile I, and profile II.

DISCUSSION OF RESULTS

General Discussion

Oscillation Sustaining Mechanisms

Considerations presented in Appendix C and elsewhere (1, 5, 7, 8, 11) establish that energy is required to sustain combustion pressure oscillations. This energy is dissipated through complicated damping processes (turbulence, heat transfer, and viscous effects) within the chamber as well as that energy lost by flow through the nozzle. The energy to sustain these oscillations is obtained from the only source available, the combustion process. Various mechanisms (1, 5, 7, 8) have been proposed by which this transfer of energy from the combustion process to the oscillating gases is accomplished. Most of these are based upon the considerations of Rayleigh (4). Rayleigh in 1896, while discussing the maintenance of oscillations by heat addition to a gaseous medium observed, "If heat be given to the air at the moment of greatest condensation, or be taken from it at the moment of greatest rarefraction, the vibration is encouraged." For any given mode of oscillation, there are discrete locations, called pressure antinodes, at which the greatest condensations and rarefractions occur (see Fig. 5). For this reason, the location of the energy addition is an influencing factor in determining which mode is more likely to occur.

In the case of the combustion chamber described herein the combustion process adds heat (energy) to the gases. Therefore, the interpretation of the above is that the oscillations will tend to be sustained if the energy

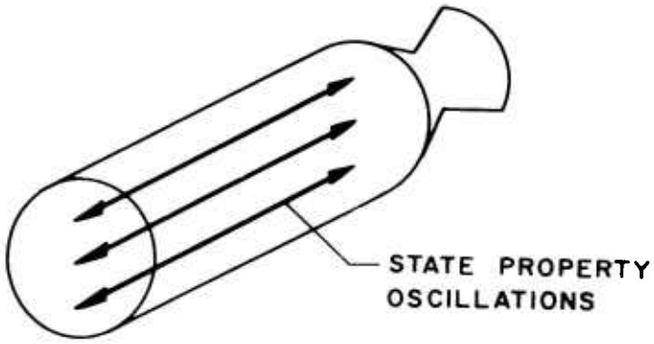

(a) LONGITUDINAL MODE

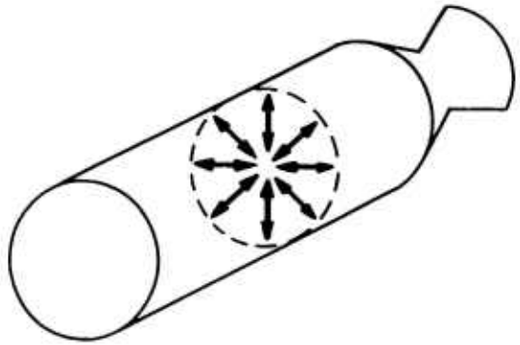

(b) RADIAL MODE

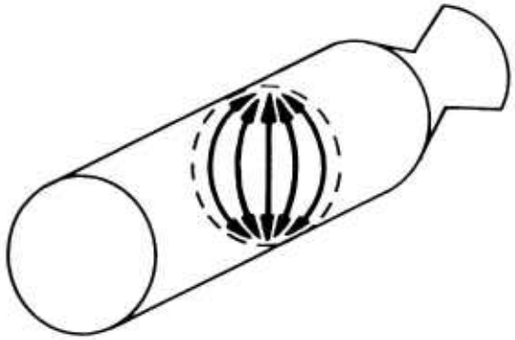

(c) SLOSHING MODE

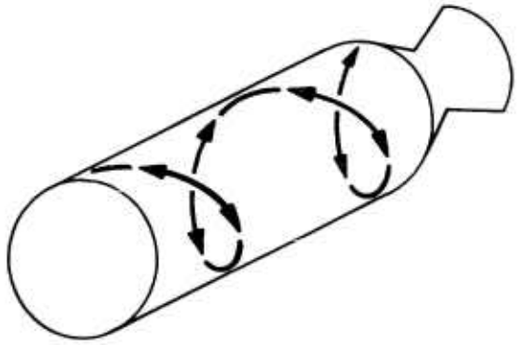

(d) SPINNING MODE

FIG. 5 MODES OF OSCILLATION

is added at the pressure antinodes of the particular mode of oscillation under consideration.

The subject rocket combustion chamber is a right circular cylinder closed at both ends (see Fig. 2). The number of modes of oscillations that might be present are shown schematically in Figs. 5 and 6. For longitudinal oscillations, the antinodal locations would be planes perpendicular to the longitudinal axis of the chamber and in various axial positions along the chamber depending upon the harmonic order. For transverse oscillations, the antinodal locations would be in various radial positions in the chamber (see Fig. 6).

Longitudinal oscillations were investigated by Davis (5) with injection (energy addition) in various axial locations, and it was found that injection near the ends of the chamber did in fact sustain the fundamental longitudinal mode. Injection near the axial midpoint, however, produced relatively stable conditions for that mode. This is in accord with the Rayleigh criterion described above (4).

The particular motor utilized in the series of experiments described herein was designed to be unstable only in the transverse modes since a 6" chamber length was selected which is below the lower critical length for the longitudinal mode (2). To facilitate the examination and discussion of the results obtained, consider the injector face as consisting of three regions A, B, and C, as shown in Fig. 7. By comparing the regions of Fig. 7 with the pressure distributions of Fig. 6, the effects of the energy released in each of the three regions can be determined by application of Rayleigh's criterion (4). Region A corresponds to the location of the pressure antinodes for oscillations of the first and second radial

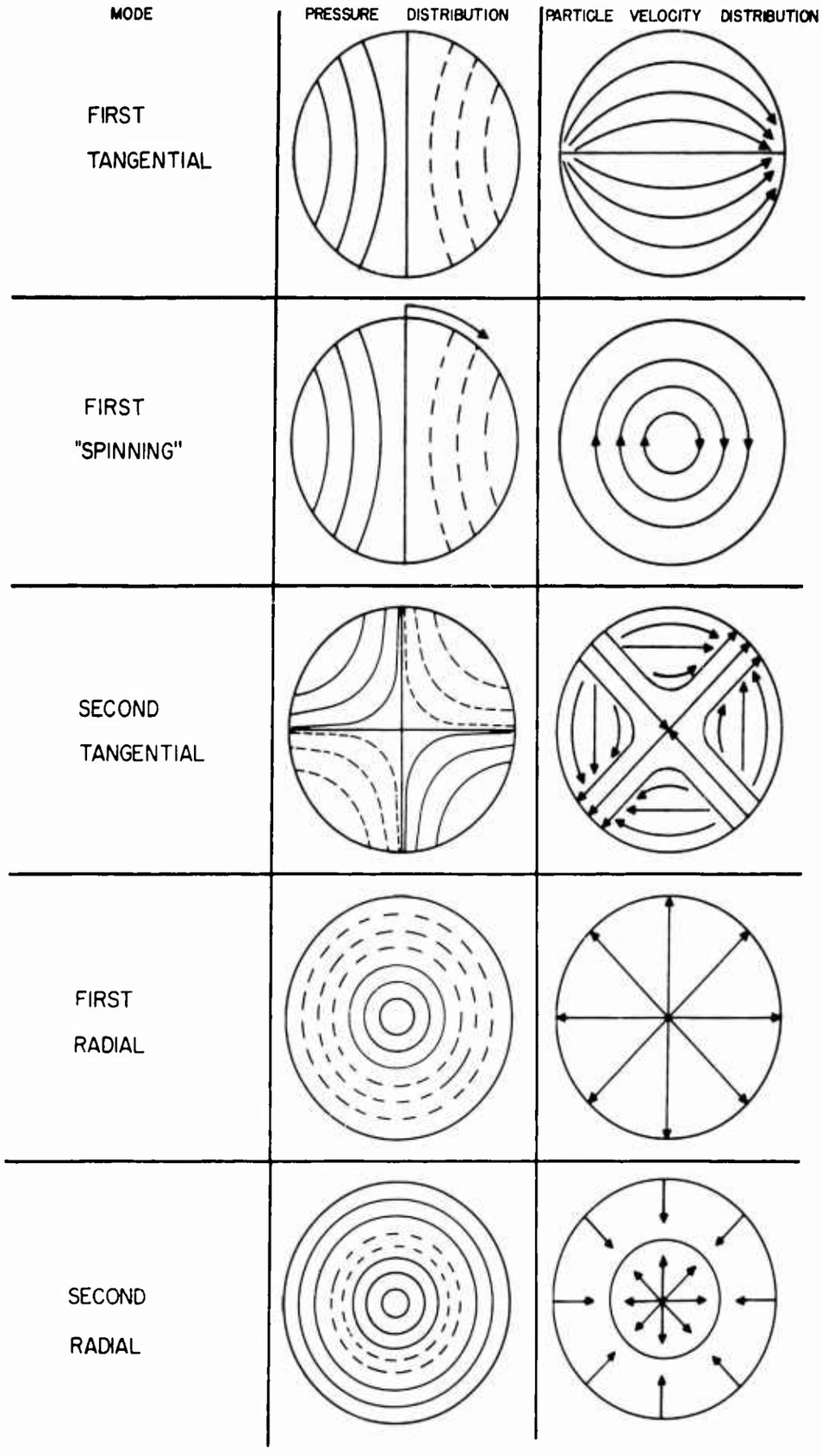

FIG. 6 THEORETICAL TRANSVERSE MODES

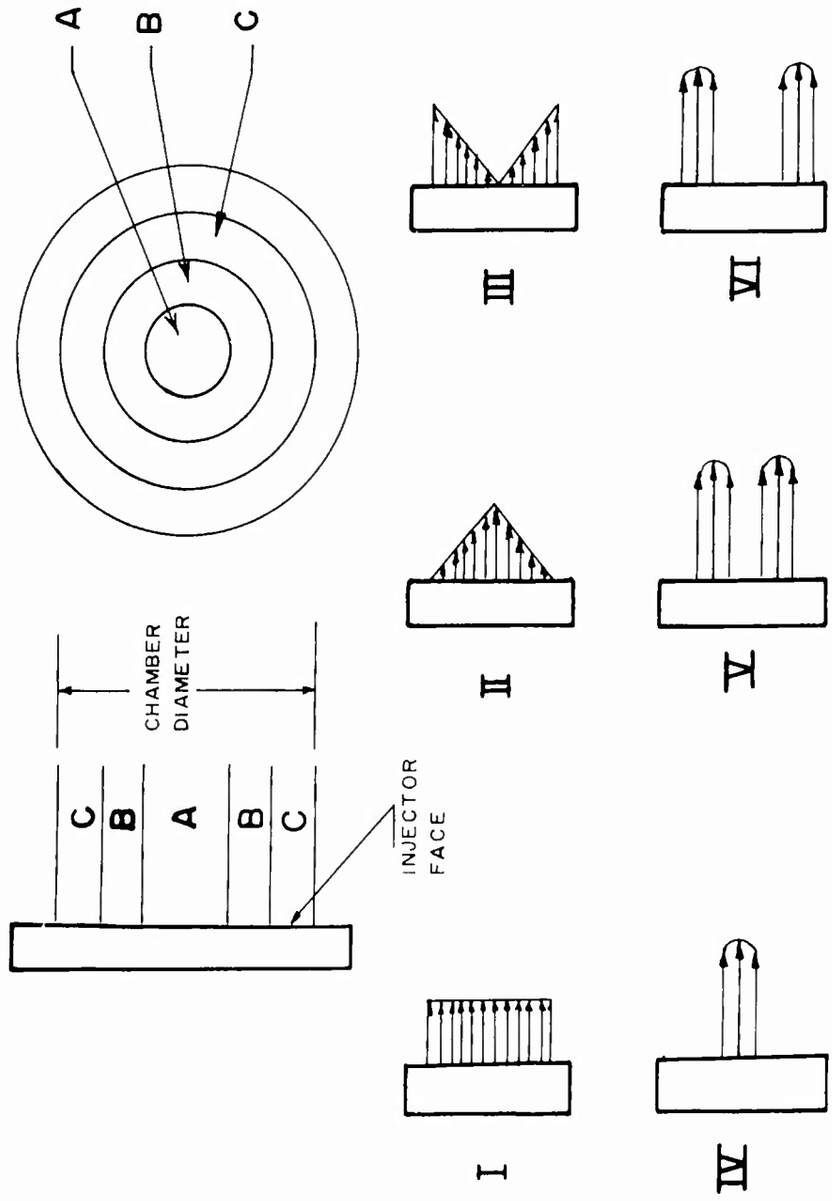

FIG. 7 INJECTION COMPARISON

modes. Thus, energy addition in region A would tend to produce oscillations of those modes. Both the radial and the tangential modes have pressure antinodes in region C. Thus, energy released at that location would be expected to sustain radial and tangential oscillations. Energy released in region B would not be at the pressure antinodal location of either type of oscillation. Thus, it would be expected to be rather ineffectual toward sustaining them.

Frequency Considerations

Equation B-3, derived in Appendix B, gives the qualitative relationship between the energy required to sustain an oscillation and the amplitude and frequency of that oscillation.

$$E \propto x_o^2 f \tag{B-3}$$

where E = energy required to sustain oscillations,

x_o = peak-to-peak amplitude of oscillations, and

f = frequency of oscillation.

References (6, 7, 8) state that a minimum initial amplitude is necessary for producing sustained oscillations and that it is independent of frequency. If then, energy is supplied to a system (at the proper pressure antinodal location) so that two oscillations of unequal frequency are initiated, a lesser amount of energy will be necessary to sustain the lower frequency oscillation than would be necessary to sustain the higher frequency mode. On the basis of equation B-3, it can then be seen that the mode having the greater amplitude would be the lower frequency one. Therefore, it can be concluded that the lower frequency modes will predominate when the energy supplied is minimal.

For example, energy released in region C would tend to drive the tangential modes as well as the radial modes. The theoretical frequency values given in Table 1 indicate that the tangential modes are of lower frequency than the radial modes. For this reason energy released in region C would tend to excite and sustain tangential but not radial oscillations. By the same reasoning, energy released in any region that would tend to excite more than one harmonic of the same type of mode would more easily drive the lower order harmonic.

Considering both location and frequency, the release of energy in region A would drive the radial mode, the release of energy in region C would drive the tangential mode, and that released in region B would be rather ineffectual.

Discussion of Results of Profiles I, II, and III

General Discussion

Several investigators in the liquid propellant rocket field (5, 7) as well as the solid propellant rocket field (11) have determined that, for a particular rocket motor configuration, the location of the energy release greatly influences the amplitude, mode, and frequency of the combustion pressure oscillations. The investigation reported herein was concerned with a rocket motor that was capable of operation with the three energy release profiles presented in Fig. 7, while the chamber geometry remained constant. It was an attempt to demonstrate clearly the effect of injection location on the transverse modes of oscillation. The following discussion is divided into that for profile I, profile II, and profile III.

Profile I

Figure 3 shows that energy release profile I resulted in oscillations of the tangential mode. These oscillations occurred between the equivalence ratios of 0.5 and 0.6 and above a mean chamber pressure of approximately 80 psia, their peak-to-peak amplitude increasing at higher mean chamber pressures and getting as high as 15 psi at a chamber pressure of 190 psia.

Profile I has an equal amount of energy released per unit area in each of the three regions; A, B, and C (see Fig. 7). Thus, by the location considerations given above, this injection pattern will supply equal amounts of driving energy to the tangential and the radial modes. As a result, the relative magnitude of the frequencies of the two simultaneously driven modes become significant. Since the tangential mode is of lower frequency, the energy supplied to it is more efficient for producing oscillations than that made available to the radial mode. Thus, the tangential mode is predominant.

Profile II

Operation with profile II resulted in essentially stable operation over the entire range of mean chamber pressures and equivalence ratios investigated even though energy is released in locations well suited for sustaining transverse mode oscillations. That is, region A receives the largest amount of the total energy released, and this energy acts to drive the radial mode of oscillation. The somewhat smaller amount of energy released in region C tends to sustain the tangential mode. The ability of either of the two modes to become predominant is dependent upon the frequency of the mode as well as the amount of energy that it receives.

Profile II balances these effects, providing a relatively large amount of energy to the higher frequency radial mode.

Thus, the distribution of energy as described above causes what can be termed an intermodal conflict between the tangential mode and the radial mode. That is, the pressure and velocity variations which occur for these modes are not compatible spatially (see Fig. 6). Moreover, since the frequencies of these two modes are unequal (see Table 1), these pressure and velocity variations are not in phase and interfere with each other. Thus, this is termed an intermodal conflict which for this particular injection system resulted in stable operation. Obtaining such an intermodal conflict may become an important means whereby liquid propellant rocket motors can be stabilized.

Profile III

Figure 4 shows that operation of the rocket motor using profile III resulted in a narrow region of unstable operation centered at an equivalence ratio of 0.6 as well as another region at higher equivalence ratios (above 1.2). The mean chamber pressures at which unstable operation occurred was above approximately 140 psia. The observed oscillations were of the tangential mode.

These results were obtained with an energy release profile that provided a large amount of energy release in region C and a somewhat smaller amount in region A. This situation is the reverse of that presented by profile II which achieved a balance between the effects of location and frequency. Profile III, however, supplies the lower frequency mode (tangential) with the majority of the energy available, and therefore, this

arrangement is more favorable for driving tangential oscillations than was profile I or profile II.

Comparison of Profiles I, II, and III

Comparison of the results of profile III with profile I disclosed that the tangential mode is driven more strongly by profile III than profile I, while the radial mode is driven less. This comparison would indicate that the predominant tangential mode of oscillation, which is common to both, should be stronger for profile III.

That this is the case can be determined by comparison of Figs. 3 and 4. In general the oscillations for a given operating point for profile III were stronger than those for similar conditions with profile I. Also, oscillations observed with profile III occurred over a larger portion of the operating range than did those of profile I.

Thus the experimental results verify the predictions based on consideration of the energy release location and the frequencies of the simultaneously excited modes.

Comparison of Results with Those of Other Investigators

Davis (5) conducted a series of experiments with the same parameters of chamber geometry and propellant combination maintained constant. The injectors employed in that program are shown schematically in Fig. 7 as injectors IV, V, and VI. Each of these three had one ring of injection holes, located at diameters of 2", 4", and 6" respectively, thereby corresponding to injection purely in regions A, B, and C.

The results obtained by (5) are in exact agreement with the observation of (4). Since these injectors did not excite two modes simultaneously, the frequency considerations previously discussed were not involved.

Injector IV, injection on the 2" diameter circle, produced instability in the radial mode. Injector V, injection on the 4" diameter diameter circle resulted in stable operation over the entire range of mean chamber pressure and equivalence ratio investigated. Injector VI, injection on the 6" diameter circle resulted in tangential oscillations.

Qualitative comparison between the results of the 6 injection profiles presented in Fig. 7 is possible because the parameters given in Fig. 1 were maintained constant for all six profiles.

To illustrate the relative instability, the maximum amplitudes of oscillation observed at a mean chamber pressure of 150 psia are given below:

Profile	Amplitude (psi)	Mode
I	7	1st tangential
II	0	----
III	11	1st tangential
IV	13*	1st radial*
V	0*	----
VI	40*	1st tangential*

* From Reference 5.

Profiles IV and VI, which each contribute energy to only one mode, produced the strongest oscillations. Profile VI drove a lower frequency mode than profile IV and thus produced stronger oscillations than did profile IV.

Profiles I and III shared their available energy between two modes and thus produced weaker oscillations than profiles IV and VI. Profile III

exhibited stronger oscillations than profile I because its energy release pattern more heavily favored the predominant tangential mode.

Observations indicate that profiles II and V produced stable operation. The reasons for this behavior were not the same in both cases. Profile V was stable because its energy was released in a location that did not readily excite either tangential or radial modes (pressure mode, see Ref. 4). Profile II, however, balanced the effects of location and frequency to produce stable operation.

Pickford and Peoples (7) discuss the fact that the combustion process provides the energy which drives and sustains combustion pressure oscillations. They indicate that the phase relationship between the energy addition and the action of the pressure wave itself is extremely important. The phase relation between the energy addition is dependent, in part, on the location of the energy release within the combustion chamber. This consideration is acknowledged by (7) when they conclude, while discussing experimental observations, that differences in propellant spatial distribution can cause variations in the inherent stability of a rocket motor.

The observations and conclusions presented herein are in agreement with the work of (7). They are an attempt to more clearly establish the nature of the differences in spatial distribution mentioned by (7). It has been observed, however, that the detrimental effects of energy release location can be countered by the intermodal action observed during operation with profile II.

Experimental work concerned with the location of energy release using solid propellants has been accomplished by Price (11). His program consisted of constructing solid propellant motors with charges made partly of

dummy propellant. The location of the burning surface was moved gradually closer to the pressure antinode of the unstable acoustic mode. The amplitude of the observed oscillations was determined to be a function of the location of the burning surface (energy release), the amplitude being the greatest when this location was coincident with the pressure antinodes.

The results of (11) are in exact agreement with those of (5). Both investigators were concerned with the location of the energy release with respect to the pressure antinode of a singular mode of oscillation. Results of the subject experimental investigation agree with those of (5) and (11) with regard to excitation of a singular mode. They also include consideration of the frequencies of oscillation if more modes than one are excited simultaneously.

The observations of (5), (7), and (11), and the results presented herein are all in agreement with the considerations of (4). While these results are significant, the other variables such as geometry, fuel composition, mixture ratio and chamber pressure should not be neglected.

CONCLUSIONS

From the results of the experiments described herein as well as the results and observations of other investigators (5, 7, 11) it may be concluded that the mode and amplitude of transverse combustion pressure oscillations are very closely related to the radial energy release variations of the injection system.

Additional conclusions were (1) Injection at the pressure antinodal location of a possible mode of oscillation will tend to excite that mode, (2) If injection under similar operating conditions in two similar rocket motors is accomplished in a manner which excites one mode in the first and a different mode in the second, the lower frequency mode will then exhibit the larger peak-to-peak amplitude oscillations, and (3) If more than one mode of oscillation is excited simultaneously, the mode and amplitude of the predominant oscillation will be determined by the frequency of each mode as well as the amount of energy supplied to each mode.

Stable operation may be achieved by the following methods: (1) The propellants can be injected at radial locations that do not coincide with the pressure antinodal locations of possible modes of oscillation and (2) The propellants can be injected in a manner that will drive two modes of approximately equal strength and the interaction between them will produce stable combustion.

BIBLIOGRAPHY

BIBLIOGRAPHY

1. Zucrow, M. J. and Osborn, J. R., "Unstable Burning in Liquid and Solid Propellant Rocket Motors," Proceedings of Bureau of Naval Weapons Missiles and Rockets Symposium, April 1961, U. S. Naval Ammunition Depot, Concord, California.

2. Osborn, J. R. and Bonnell, J. M., "An Experimental Investigation of Transverse Mode Combustion Oscillations in Premixed Gaseous Bipropellant Rocket Motors," Purdue University Report No. I-60-1, January 1960.

3. Ross, C. C. and Datner, D. P., "Combustion Instability in Liquid Propellant Rocket Motors - A Survey," Selected Combustion Problems - Fundamental and Aeronautical Applications, Butterworths Scientific Publications, 1954.

4. Rayleigh, J. W. S., Theory of Sound, Vol. II, Dover Publications, 1945, p. 226.

5. Osborn, J. R. and Davis, L. R., "Effects of Injection Location on Combustion Instability in Premixed Gaseous Bipropellant Rocket Motors," Purdue University Report No. I-61-1, January 1961.

6. Schiewe, R. M., "An Experimental Investigation of High Frequency Combustion Pressure Oscillations in a Gaseous Bipropellant Rocket Motor," M. S. Thesis, Purdue University, June 1959.

7. Pickford, R. S. and Peoples, R. G., "The Inherent Stability of the Combustion Process," ARS Preprint 1490-60, ARS 15th Annual Meeting, December 1960.

8. Crocco, L. and Grey, J., "Combustion Instability in Liquid Propellant Rocket Motors," Proceedings of Gas Dynamics Symposium, Northwestern University, 1956, pp. 55-70.

9. Osborn, J. R., "An Experimental Study of Combustion Pressure Oscillations in a Gaseous Bipropellant Rocket Motor," Ph.D. Thesis, Doc. I, Purdue University, June 1957.

10. Church, A. H., Mechanical Vibrations, John Wiley and Sons, Inc., 1957.

11. Price, E. W., "Analysis of Results of Combustion Instability Research on Solid Propellants," ARS Preprint 1068-60, ARS Solid Propellant Rocket Research Conference, January 1960.

APPENDICES

APPENDIX A

NOTATION

Symbol	Explanation	Units
A	area	$inch^2$
c	viscous damping coefficient	lb_f-sec per inch
C	compressibility factor	none
C_T	correction factor	none
cps	cycles per second	cycles per sec
E	energy	ft-lb_f
E.R.	equivalence ratio	none
f	frequency	cycles per sec
F	flow factor	none
F_o	force	lb_f
H	number of holes	none
k	spring constant	lb_fper inch
K	orifice constant	none
m	mass	slug
p	mean static pressure	lb_fper $inch^2$
P_c	mean chamber pressure	lb_fper $inch^2$
psia	pounds per square inch, absolute	lb_fper $inch^2$
R	degrees Rankine	degrees Rankine
t	time	sec
T	temperature, absolute	degrees Rankine

Symbol	Explanation	Units
$\dot{w}$	flow rate	lb_m per sec
x	displacement	inch
$\dot{x}$	dx/dt	inch per sec
$\ddot{x}$	d^2x/dt^2	inch per sec^2
x_o	peak amplitude of oscillation	inch
Y	expansion factor	none
γ	specific weight	lb_m per $foot^3$
π	3.14159	none
ω	angular frequency	rad per sec

APPENDIX B

FUNCTIONAL RELATIONSHIP FOR SUSTAINING ENERGY

In the discussion of the combustion pressure oscillations observed in this experimental investigation, the effect of frequency upon the energy required to sustain the oscillations is introduced. There is no relationship available in the literature that relates these two variables. This situation is due to the nonlinear nature of the damping processes and the fact that the nature of the damping processes (turbulence, radiation, viscosity) is not clearly understood.

Consider the situation present in a rocket motor operating with high frequency combustion pressure oscillations. Within the chamber there exists an oscillating system. That is, the gas particles in the combustion chamber have an oscillatory motion superimposed upon the steady flow motion. The unbalanced pressure within the chamber is the driving force which causes the particles to oscillate. This driving force acts against the inertial forces which are due to the momentum of the particles. Moreover, the oscillations will die out if energy is not supplied to them; thus, some sort of damping forces are present.

Basically then, three elements exist which are analogous to the three elements of a simple lumped parameter, mass, spring, and damper system.

The gases themselves constitute the mass, the unbalanced pressure is analogous to the spring and the damping processes mentioned above are similar to those processes which occur in the viscous damper. Certainly

the analogy is not very strong as the character of each of the elements vary between the two systems. For this reason caution must be used when drawing conclusions based upon it. However, the analogy will be used to help establish a functional relationship which successfully aids in the explanation of combustion pressure oscillations.

The equation of motion of the simple lumped parameter mechanical system is (10):

$$m\ddot{x} + c\dot{x} + kx = F_o \cos \omega t \qquad \text{(B-1)}$$

where m = mass,

$\ddot{x}$ = second time derivative of x,

c = viscous damping coefficient,

$\dot{x}$ = first time derivative of x,

k = spring constant,

x = displacement, and

$F_o \cos \omega t$ = sinusoidal driving force applied to m.

The amount of energy put into such a system may be obtained by taking the product of the force applied and the displacement of the force and then integrating the product over a time interval equivalent to one cycle. The resulting equation is (10):

$$E = - 2\pi^2 c x_o^2 f \qquad \text{(B-2)}$$

where E = energy transferred,

c = viscous damping coefficient,

x_o = peak displacement,

f = frequency of oscillation,

and where the minus sign merely indicates that the energy is being put into the system, obviously an equal amount is dissipated.

Due to the weakness of the analogy, equation B-2 cannot be taken as the equation which describes the energy addition to an oscillating gaseous medium, but on the basis of the fact that both systems are forced oscillating systems, the following functional relationship is applicable to either:

$$E \alpha x_o^2 f \qquad \text{(B-3)}$$

where the terms are the same as they were in equation B-2. Because equation B-3 is a functional relationship, the x_o term represents either the peak displacement from the midposition or the peak-to-peak amplitude, these two displacements differing by a factor of 2.

Equation B-3 describes the manner in which the energy necessary to sustain oscillations in a rocket combustion chamber is dependent upon the amplitude and frequency of these oscillations. It shows that the energy required to sustain a larger amplitude of oscillation varies with the square of the peak-to-peak amplitude while this energy requirement is only a first power function of frequency.

When considering the oscillations in a rocket combustion chamber, several different modes of unequal but rather well defined frequencies are possible. An interesting situation arises when the amount of energy made available to drive an existing oscillation is increased. Two possibilities exist, the amplitude may increase or the frequency may shift to that of a different mode or perhaps a higher harmonic of the existing mode. In the

event of a mode shift the amplitude may change slightly to satisfy the function relationship of equation B-3.

APPENDIX C

DESCRIPTION OF APPARATUS

General Description

The test cell, control room, propellant feed system and instrumentation are fully described in Reference (5).

Figure 8 is a cross sectional view of the rocket motor utilized in this series of experiments. The motor consists mainly of 4 components; the premixer, the injector, the combustion chamber, and the nozzle.

The Combustion Chamber

The combustion chamber is an uncooled right circular cylinder with a 7" inside diameter and 6" axial length. It is constructed of mild steel with mounting flanges welded to each end to receive the injector plate and the nozzle plate. Tapped holes are provided in the chamber wall for the transducers, mean chamber pressure tap and post run chamber coolant.

The Nozzle Plate

The nozzle plate was a mild steel plate with a DeLaval nozzle with a 0.5" throat diameter welded to it. The converging-diverging portion of the nozzle was constructed of stainless steel. The converging and throat portion was convectively cooled with water and the diverging portion was cooled by external cooling tubes. An automotive type spark plug was installed in the nozzle plate to provide ignition.

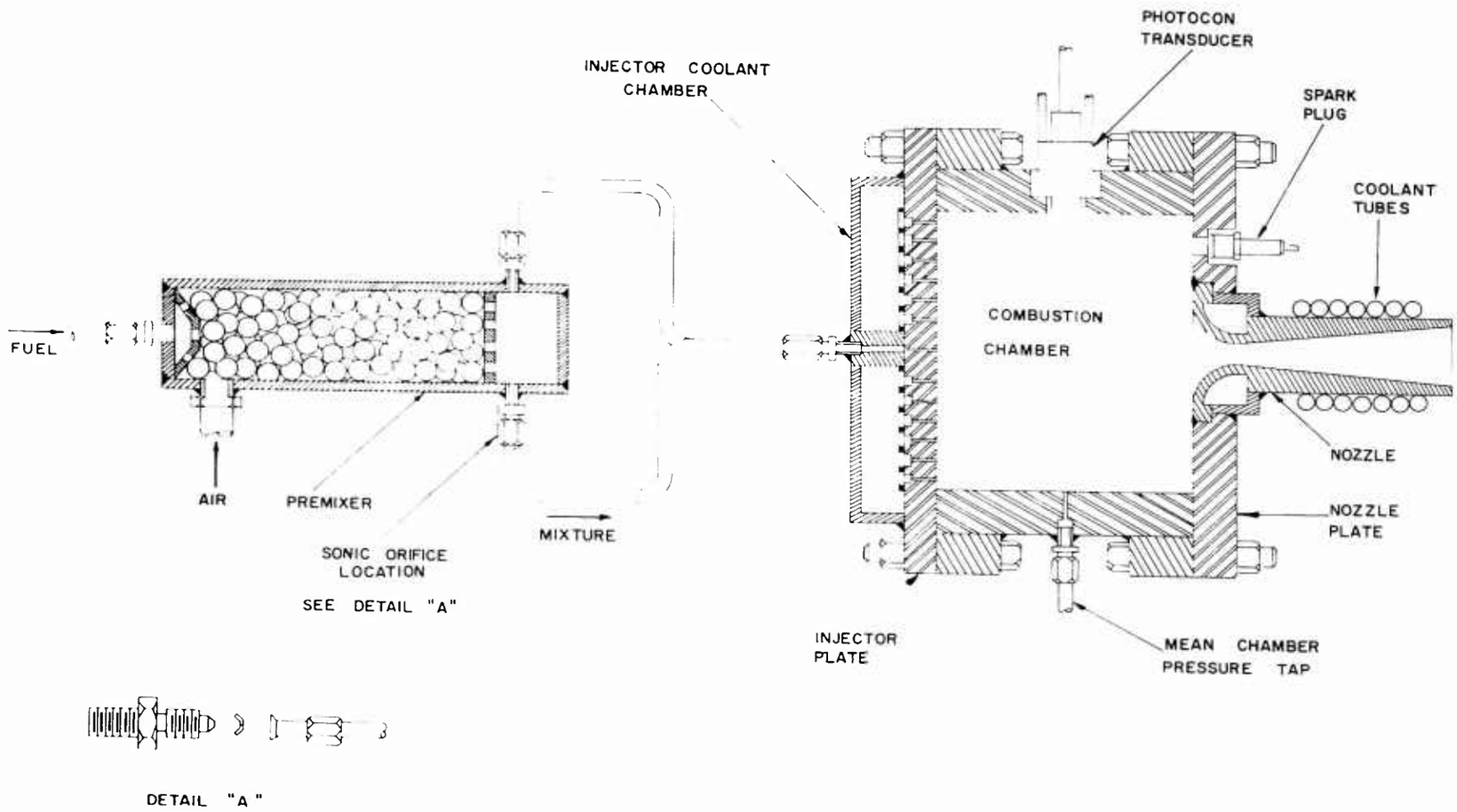

FIG. 8 SECTIONAL VIEW OF RESEARCH ROCKET MOTOR

The Premixer

The premixer was a stainless steel chamber filled with two hundred and twelve 1/2" diameter brass balls as shown in Fig. 8. The fuel and oxidizer enter and pass through the packed balls, thus being thoroughly mixed. The mixed propellants then flow through seven lines to the seven concentric rings of injection holes in the injector plate.

The Injector Plate

The injector plate, shown in Fig. 9, was convectively cooled on its exterior surface. The injection hole pattern shown in Fig. 10 consists of seven concentric rings of holes, spaced such that each ring was centrally located in one of the circular strips of injector face shown in Fig. 10. These rings are denoted as ring numbers 1, 2, 3, 4, 5, 6, and 7. The areas are in the ratios of 1, 3, 5, 7, 9, 11, and 13 and thus the rings have 1, 3, 5, 7, 9, 11, and 13 holes respectively. The holes were arranged radially at random in an effort to avoid local concentrations of holes and thus energy release.

Each ring of injection holes issues from a manifold machined into the upstream side of the injector plate. Bosses welded to these manifolds receive the lines from the premixer. The two outermost manifolds each have two bosses to reduce the possibility of a sizeable pressure drop within these manifolds causing an uneven distribution of propellant to each hole.

Flow Metering Orifices

The premixer and the injector were connected by seven 1/4" stainless steel lines. Each line contained a small brass orifice (shown in Fig. 8)

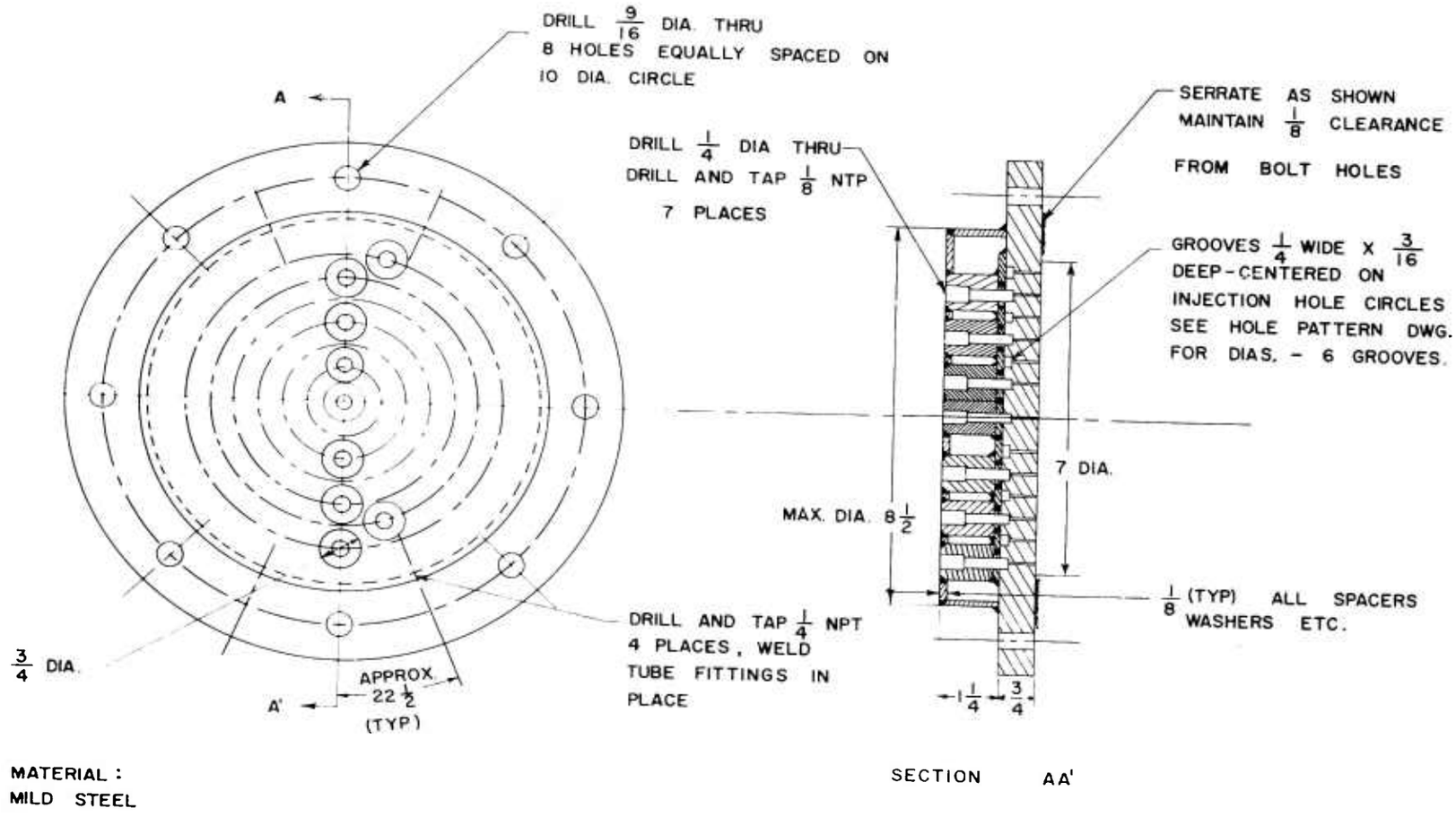

FIG. 9 INJECTOR PLATE

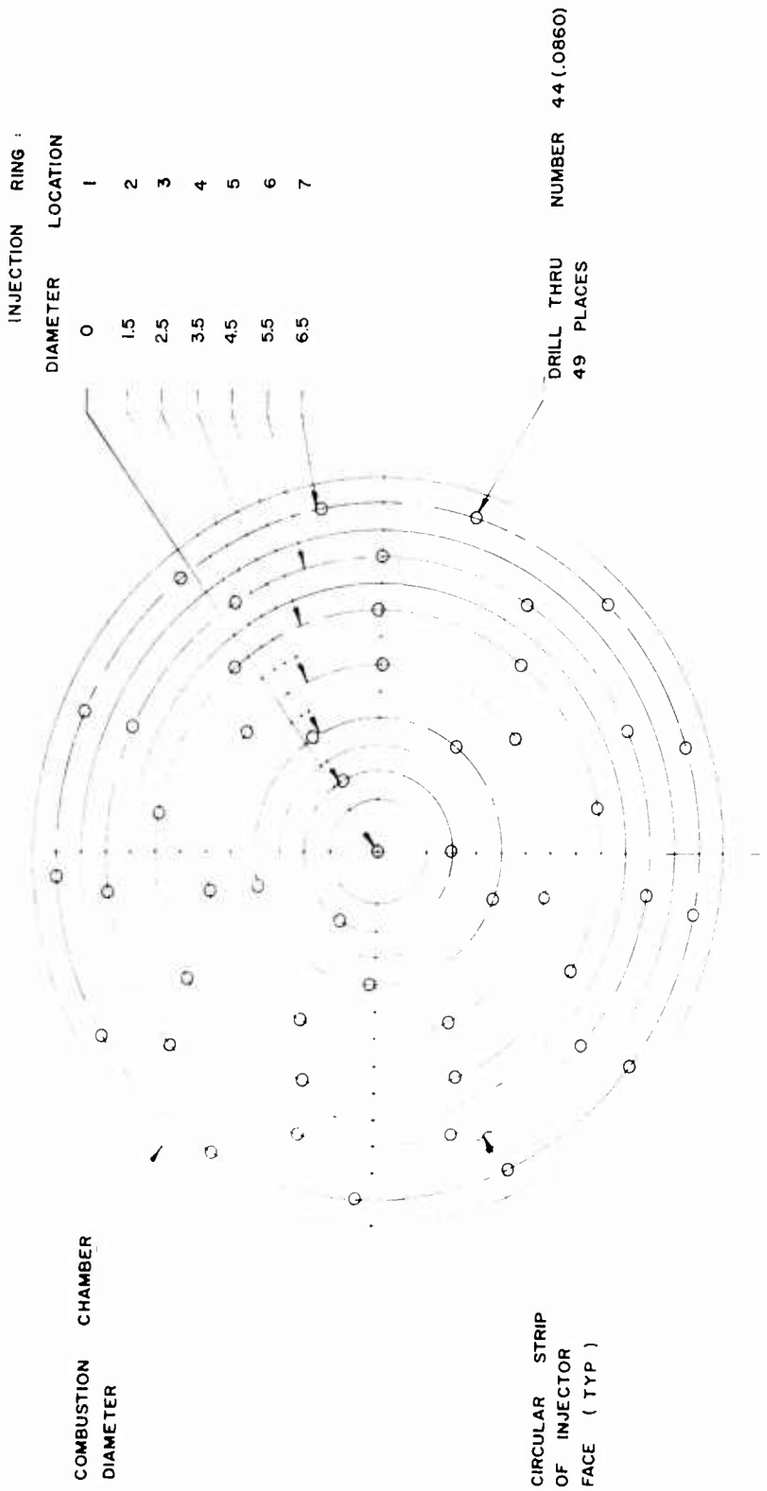

FIG 10 INJECTION HOLE PATTERN

at the premixer end, that became choked during operation. Since the orifices were choked, the fraction of the total propellant flow that passed through each one was a function of the upstream conditions, which were common to all orifices. Thus, the flow rate became a function of the size of the orifice only.

In order to eliminate the possibility of various discharge coefficients affecting the selection of orifices on an area basis, a large number of orifices were constructed and checked with the air flow rate necessary to cause choking while maintaining constant upstream conditions. The values of flow rate thus acquired were then used to determine which combination of orifices would most closely develop the desired profiles.

For each profile, factors were assigned to each ring of injector holes corresponding to the relative amount of energy to be released at that location. These factors are shown graphically in Fig. 11. This factor was multiplied by the number of holes at each location and the orifices for each location were selected so that

$$\frac{\dot{w}_i}{\sum \dot{w}_i} = \frac{H_i F_i}{\sum H_i F_i} \quad (i = 1 \rightarrow 7) \tag{C-1}$$

where $\dot{w}_i$ = calibration flow rate of $i^{\underline{th}}$ orifice,

H_i = number of holes in $i^{\underline{th}}$ location, and

F_i = factor of $i^{\underline{th}}$ location.

The values of flow rate for each orifice and the arrangement of orifice combinations for each profile are given in Tables 2 and 3 of Appendix E.

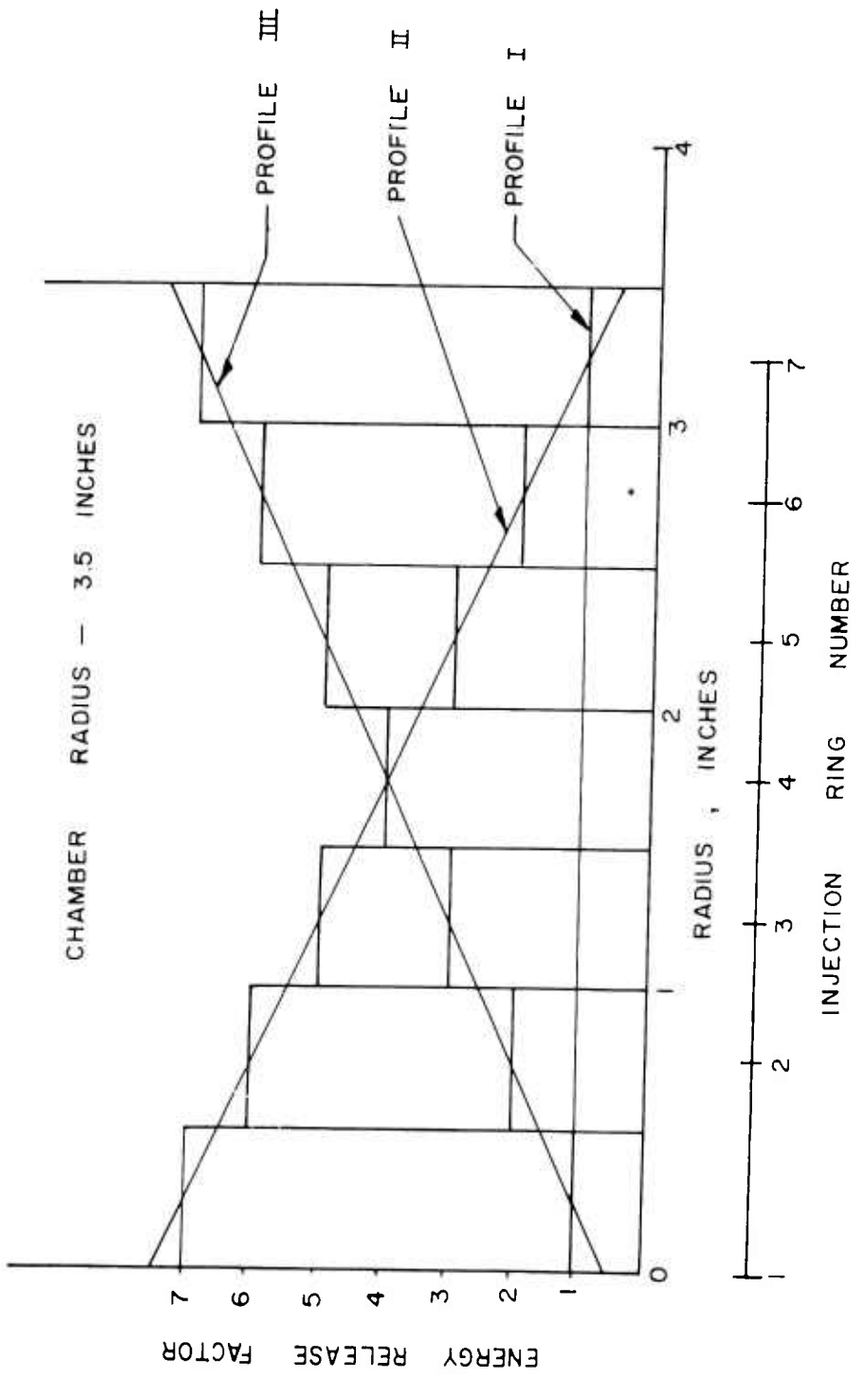

FIG. 11 PROFILE FACTORS

APPENDIX D

METHOD OF EVALUATING DATA

The output signal of the Photocon-Dynagage system was simultaneously viewed by the operator on an oscilloscope and recorded at 60 inches per second on an Ampex tape recorder. After the run, while the tape was replayed at 1 7/8 inches per second, the signal was fed into the Hathaway oscillographic recorder. By comparison of the incident signal with a calibration signal of known frequency and amplitude, the frequency and amplitude of the pressure oscillations were determined.

Calculation of the flow rates of each of the propellants was accomplished by employing the following equations:

$$\dot{w}_{std} = 0.668\ KAY\sqrt{\gamma \Delta P} \qquad \text{(D-1)}$$

where $\dot{w}_{std}$ = flow rate,

K = orifice flow constant,

A = area of the orifice,

Y = orifice expansion factor,

γ = specific weight,

ΔP = metering orifice pressure drop

and $\dot{w}_{std}$ and γ are based on an upstream temperature of 520°R and the assumption that the gas follows the perfect gas law. The following correction factor was used to correct the flow rate determined by equation D-1.

$$C_T = \sqrt{\frac{520^\circ R}{T_x}} \sqrt{\frac{1}{C}} \qquad \text{(D-2)}$$

where C_T = correction factor,

T_x = actual upstream temperature, and

C = compressibility factor.

Therefore,

$$\dot{w} = C_T \dot{w}_{std} \qquad \text{(D-3)}$$

where $\dot{w}$ = actual flow rate.

The equivalence ratio was determined by dividing the actual fuel-oxidizer ratio by the stoichiometric fuel-oxidizer ratio for the propellant combination.

The mean chamber pressure was obtained directly from an Esterline-Angus Bourdon tube type pressure recorder. Addition of atmospheric pressure converted this reading from gage pressure to absolute pressure.

"Distribution of this report has been made in accordance with the Joint Army-Navy-Air Force Liquid Propellant Mailing List of December 1961."